

Abstract

In Exercise 1 a simple cuboidal water bath with a point fission source of $10^{10}s^{-1}$ neutrons was modelled. The average flux was recorded as $(3.44882 \pm 0.00344882) \times 10^7 s^{-1}$ on the surface nearest to the source (base of the tank) and $(2.509440 \pm 0.00677549) \times 10^6 s^{-1}$ on lateral sides of the tank furthest from the source.

In Exercise 3 a cubic water bath with five enriched uranium cylinders was found to have a $k_{\text{eff}} = 1.01798 \pm 0.00046$ when $e=20\%$; in order to keep the set-up safe, defined by $k_{\text{eff}} < 0.8$ when $e=25\%$, ≥ 0.139804 wt.% boron is required in the water.

1 Introduction

See the Appendices for the geometries and materials definitions of the following problems.

1.1 Exercise 1: Simple Neutron Source in a Bucket of Water

A narrow, stainless steel water bath is subjected to a point source of (uranium thermal fission) neutron near its bottom. The neutron fluences and spectra measured just outside each of the faces of the neutron bath are examined.

1.2 Exercise 3: Criticality

A square water bath with four short, fully-submerged enriched Uranium cylinders, arranged in a “plus” sign, is shown to be supercritical when moderated by pure water, even when it is only enriched to $e=20\%$. The aim of the exercise is to find the minimum degree of boronation in the water required to keep the system subcritical to $k_{\text{eff}} < 0.8$ when the cylinders are enriched to $e=25\%$.

2 Method

2.1 Technicalities for reproducibility

Software and hardware specifications For the following exercise all cross-section data were retrieved from the ENDL92 library (the most recently updated library available, acquired by Lawrence Livermore National Laboratory) and simulated in MCNP 4C2, ran on the phymat server of University of Birmingham School of Physics and Astronomy, which is a Scientific Linux 7.3 (Nitrogen) system with 16 CPU's (Intel(R) Xeon(R) CPU E5-2630 v3 @ 2.40GHz) (though only 1 CPU is used at a time).

Reproducibility of the .ip files In both cases, the default random number control 0.727343232450560E+14 was used, and the centre of the stainless steel tank's exterior surfaces was placed at the origin.

Material definition The isotopic composition of water was retrieved from [4]; the elemental composition of other materials were provided by the problem sheet, and were all assumed to have the same isotopic compositions as naturally occurring elements stored by the default AAA=000 option in the ZAIDs identifier. See the tables in the Appendices for more.

Geometry definitions The geometries for exercise 1 and 3 were set to the dimensions as required by the problem sheet; the cross-sections of their geometries are shown in Figure 2 and 3 in the Appendices. Note that all voids within the re-entrant surfaces were allowed to have neutron importance =1 to allow re-entry of the neutrons into solid components without “killing” the neutron.

Energy cutoff Energy cutoff is not applied so that very slow (thermalized) neutrons are allowed to interact and let further reactions take place.

2.2 Exercise 1

Tallies Therefore for exercise 1, the lower bound of the 1st bin of each tally is $E=0$.

The temperature of the cross-section data in database 42(ENDL92) were acquired at $T=300\text{K}$, as shown in 91-99, and is subsequently adjusted down to 20.4°C ($2.53 \times 10^{-8}\text{MeV}$) when running the simulation. Either way, thermal effects should significantly affect that falls into the first 3 energy bins. ($0-10^{-9}\text{MeV}$, $10^{-9}-10^{-8}\text{MeV}$, $10^{-8}-10^{-7}\text{MeV}$ respectively).

The tally probability distributions (histograms shown in table 161) all show reasonably Gaussian distributions (and the cumulative probability distributions all show reasonably sigmoidal distributions) without the majority of the counts falling into a single bin; therefore there is no inherent need for using a finer spacing; but for the purpose of visualizing the spectrum with a higher resolution, a finer group structure with trifolled bin density (still logarithmically spaced, 3 bins per decade) was used.

Even when the spacing of energy groups is trisected in this manner, the 1st bin (0 to $1 \times 10^{-9}\text{MeV}$) is still the bin that receives the least counts. In a real problem this would have been merged with the 2nd bin to form a single, larger bin to tally up all the completely thermalized neutrons, increasing its count so that it converges to a precise enough value in a shorter CPU time; but according to the constraint of the problem, there must be

one bin with 10^{-9} MeV as the upper limit. Therefore the only option left is to increase the number of histories such that the results of this bin converges.

Number of particles Due to the large cross section in the thermal region which increases as the neutron slows, very few neutrons of these energies can travel far enough to be counted by these surface flux tallies. Therefore this bin always have the largest relative errors among all bins. To ensure that no bins have relative error larger than 0.10 such that the results are reliable, enough histories must be ran to allow the 1st energy bins in all 3 tallies to be filled sufficiently, in addition to passing all 10 statistical checks.

The number of particles required is discussed in detail in section 4.1.1.

Source location By examining the first 50 particles(using PRINT 110), the source was confirmed to be an isotropic point source 2cm above the centre of the bottom of the tank's internal surface; and the majority of the particles have initial energy $E < 4$ MeV as expected when they are distributed according to the Watt spectrum for neutron generated by $^{235}\text{U} + n(\text{thermal})$ (See the Watt spectrum in Figure 4).

2.3 Exercise 3

Note on cross-section library There is no delayed neutron cross section data available in ENDL92 (or any other nuclear databases available on phymat), so the simulation may deviate from reality slightly. There is no workaround for this issue; but one can assume, for the purpose of this simulation, that a cross-section database without delayed neutron cross-section should be accurate enough.

Geometry definition It is easier to define the geometry if a sphere was used to define the graveyard (void) outside (where neutron importance=0); but a cuboidal geometry was chosen instead to allow the surface flux detectors (F2) to tally particles passing through lateral surfaces separately from particles passing through the horizontal surface.

All components except the concrete floor had the same neutron importance. Neutron importance in concrete was initially set at 1 but was subsequently reduced to 0.1 such that the simulation runs faster by ignoring particles that enter the concrete, since they will otherwise undergo a lot of collisions (each adding to the computing time) to slow down, without reflecting back into the U cylinders to cause more multiplication.

If the mean free path to absorption λ_{abs} is known, the dimension of the concrete floor can be chosen to extend from the stainless steel tank by $N\lambda_{\text{abs}}$ where N is some arbitrary threshold factor (e.g. N= 3). However only the mean free path to *collision* for neutron is found on a cell particle activity table (using PRINT 126). Since concrete is only a weakly neutron-absorbing medium, this *cannot* be used as the proxy for λ_{abs} . Instead the fraction of neutrons escaping the concrete block into the void was measured. This was done by comparing the number of neutrons travelling from the concrete to the void region (where neutron importance = 0) (measured with a surface flux tally card) to the neutron population in the concrete. The quantity “population” instead of “tracks entering” was used because the latter re-counts particles re-entering the same cell, thus the former is a more accurate measurement of how many distinct neutrons have been present in the concrete block. The simulation is considered accurate when the ratio of these two numbers is less than 1%, i.e. $< 1\%$ of the neutrons entering the concrete were “killed” (by entering the void region) instead of being absorbed in the concrete/reflected back towards the tank. The dimension of the concrete block was increased until this ratio is lower than 1%.

This resulted in a concrete floor block of 160.4cm in the x- and the y-directions and 50 cm in the z-direction, resulting in 0.21621209% and 0.04494092% of neutrons escaping through the lateral planes and the horizontal plane (plane separating the concrete block from the void below) respectively. Therefore this was used as the final dimensions for the concrete block.

Source definition Using the KSRC card a “generic Watt spectrum”[1] of neutrons were created at the centre points of each cylinder.

This allowed for very fast convergence of the results, where the k_{eff} value settled down to a stable value in less than 10 generations. The k_{eff} estimation started after that.

The alternatives of using an SDEF card with a cookie cutter(CCC) rejection/CEL rejection, and using 5 uniform cylindrical sources overlayed onto cell 11-15 (all the uranium cylinder cells) were attempted, but were not applied in the end because it is likely to distribute neutrons close to the non-re-entrant surfaces where they can escape, reducing the effectiveness of the source and potentially increasing the number of cycles that needs to be skipped. [2]

Choices of number of particles and number of cycles 3000 particles per cycle were shown to give a k_{eff} that converges in ≈ 10 cycles; 5000 particles per cycles were shown to give faster convergence of k_{eff} value (in < 5 cycles), but further increase in number of particles per cycles to 8000 did not show significant improvement in speed of convergence. Therefore the number of particles were chosen to be 5000, and to be servative, the first 10 cycles were skipped (IKZ=10).

At 5000 particles per cycle, k_{eff} was shown to converge sufficiently by the 500th cycle; further increase in total number of cycles yields deminishing marginal increase in precision at the cost of increasing the computing time, asymptotically approaching 0; thus only 500 cycles were ran, requiring 10.27 minutes of computing time.

The number of cycles to run per simulation were later changed when the k_{eff} changed. For details see section 4.2. As for the initial guess of k_{eff} it was kept at 1 for all cases. (RKK=1)

Alteration to the material definition For ease of changing the input file, when attempting to find a concentration of boron that gives a solution, the excess boron is added *on top of* the existing weight fractions for hydrogen and oxygen, the latter two already summed to unity. This results in a weight fraction of boronated water with larger-than-unity, unnormalized weight fraction; and only this excess weight fraction of boron was changed between iterations, allowing MCNP to calculate the normalized weight fraction of boron in water before running each simulation. The resulting, correctly normalized weight fraction of boron is printed in table 40.

3 Result

3.1 Exercise 1

See table 1 below for the fluences on each surface. In the Appendices, figure 5 shows the spectra of neutron energies at the three tallying surfaces; The tally fluctuation chart is plotted in Figure 7 (and Figure 6 for the same plot with a linear y-axis scale). Additionally the figure of merit variation is plotted on Figure 8.

3.2 Exercise 3

The k_{eff} variation by cycle is plotted on Figure 9, including the 1σ confidence interval. In particular, the k_{eff} for 20wt.% enriched uranium with no boron addition is reported (in line 4174-4178 of the output file) as “the final estimated combined collision/absorption/track-length $k_{\text{eff}} = 1.01798$ with an estimated standard deviation of 0.00046 the estimated 68, 95, & 99 percent k_{eff} confidence intervals are 1.01752 to 1.01843, 1.01707 to 1.01888, and 1.01677 to 1.01918”

As for the case where the uranium is enriched to e=25% and a minimum boron concentration of 0.139804wt.% is added to the water, to keep $k_{\text{eff}} < 0.8$, the following result:

“ $k_{\text{eff}} = 0.79766$ with an estimated standard deviation of 0.00033 the estimated 68, 95, & 99 percent k_{eff} confidence intervals are 0.79732 to 0.79799, 0.79699 to 0.79832, and 0.79677 to 0.79854” is reported.

The variation of k_{eff} wrt. Boron concentration is given in table 5 in the Appendices.

4 Analysis and discussion

Note:from the Watt spectrum (Figure 4) that there is a small but non-zero probability of getting neutrons of very high energy. This leads to some warning messages when the occasional particle scores above the upper limit of the largest tallying bin in Exercise 1.

4.1 Answer to numbered questions for Exercise 1

1. For the 20,000 particles case, its results have limited reliability because the last statistical check (pdf slope=decreasing?) for tally 22 and 32 were not passed, meaning that some reactions are not sampled enough for us to be confidence about the frequencies of their occurrence. Additionally, some bins in the PDF are empty (seen in table 161 of tally 22) suggesting that insufficient number of neutrons is sampled to approximate a continuous distribution.

However, for the 2,800,000 particle case, the results are reliable as they have passed all statistical tests. Regardless, the one should be aware that these results are the fluences AVERAGED over the entire tallying surface. The centre points of each surface are subjected to a higher-than-average fluence while the corners experiences a lower-than-average fluence.

2. Using the notation of

Φ_i = fluence calculated for the i^{th} energy bin *per history*, (nps) = number of histories

tally (surface(s))	12 (long sides)	22 (short sides)	32 (base)
fluence (cm^{-2}) for nps= 20000	15.0 ± 0.2	4.80 ± 0.16	68.5 ± 0.8
fluence (cm^{-2}) for nps= 2800000	2151.4 ± 2.2	702.6 ± 1.9	9656.7 ± 9.7

Table 1: The total fluences Φ after the whole simulations are simply calculated by formula $\Phi = N \sum_i (\Phi_i)$, unit = $1/\text{cm}^2$

3. In both the nps=20,000 and nps=2,800,000 case, the spectra and the mean energy of the tallies reflects

that the hardness of neutron spectrum decreases with distance: hardness at base (Tally 32)>long side (Tally 12)>short side (Tally 22), as can be seen from Figure 5 and 6.

There is a noticable increase in number of thermalized neutrons with $< 10^{-7}\text{MeV}=0.1\text{MeV}$ as distance increases, while the prompt neutrons with energy $> 0.1\text{MeV}$ decreases. This is because neutrons gets slowed down/captured after travelling through more water; and the slower it is the more likely that it will be removed from the current energy group, as shown by the total interaction cross sections plotted in Figure 10. This effect dominates until it reaches thermal temperature, where up-scattering occurs.

More neutrons can penetrate the base at the energy its creation energy without being moderated by the water; therefore the 1st bin of tally 32 is more filled than that of tally 12.

The fluence also decrease in the same order as a result of the inverse square law and the capture of neutron by water when they have to travel through a longer distance in water.

4.1.1 Number of histories required to converge

Even after running 500,000 histories, the relative error for this 1st bin remains high (0.2599, 0.4236, 0.3681, for tally 12, 22, and 32, respectively) despite the fact that all other statistical checks were passed after running 500,000 histories, and the FoM has already converged to a reasonably stable asymptotic limit.

If one does not care for the accuracy of the 1st bin, then running 2,800,000 histories is sufficient, as it passes all statistical test, and produces a sufficient number of dancing, in a reasonable computing time of 1.98 minutes; and all bins (except the first) will have fractional errors < 0.1 after this many histories. Therefore the results from that simulation (nps=2,800,000) was used for plotting all graphs in the Appendices.

However, 18,000,000 histories are required for the convergence of all of the 1st bins, requiring 12.78 minutes of computing time, which is quite long for a simple problem. And even after 18,000,000 histories, only a limited number of neutrons arrive at the surfaces for tally 22, leading to a fluctuating Figure of Merit being recorded, resulting in what appears to be a decreasing trend in FoM the last half of the simulation, missing the last statistical check. Therefore the result of this bin is less reliable than the result of the rest of the bins concerned.

4.1.2 10^{10} n./s conversion factor

If this simulation is meant to represent a 10^{10}s^{-1} neutron source, then a multiplication factor of $= 10^{10}\text{s}^{-1}$ should be multiplied onto the normalized neutron flux values given in the output file, giving

tally (surface(s))	12 (long sides of the tank)	22 (short sides of the tank)	32 (base of the tank)
Flux ($\text{cm}^{-2}\text{s}^{-1}$)	7683410 ± 7683	2509440 ± 6775	34488200 ± 34488.2

Table 2: Flux expected from a 10^{10}s^{-1} point source of neutron placed at the same location, predicted from the 2,800,000 neutrons simulation. See table 4 in the Appendices for the full table including the fluences predicted using the other two simulations' results as well.

4.2 Answer to numbered questions for Exercise 3

1. The final k_{eff} estimate and its standard deviation is reported for 20wt.% enriched uranium with no boron addition as 1.01798 ± 0.00046 (See section 3.2)

The average combined k_{eff} (blue line (c/a/t) in the Figure 9) was observed to decrease slightly at the beginning, converging onto and the value of 1.01798, and then stabilize around this value, with decreasing standard deviation as the simulation progresses and sample size increase.

2. The final results of $k_{\text{eff}} = 1.01798 \pm 0.00046$ is fairly reliable, considering the following items, as suggested by [3]:
 - all cells with fissile isotopes (i.e. all U cylinders) were sampled
 - the average combined k_{eff} appeared to be varying randomly about the average k_{eff} for the average cycles
 - no noticable trend was present in the later stage of the average combined k_{eff}
 - the confidence intervals from the batched combined k_{eff} does not appear to differ significantly from the final result, meaning there are no cyclic variations
 - the Figure of Merit for combined k_{eff} is stable.

and lastly,

3. when assessing the safety of the subcritical set-up, one should also account for
 - breeding of more fissile material as the reaction progresses (the U-238 absorbing neutrons and transmuting into Pu-239),

- any nearby similar structures that may reflect/produce neutrons, e.g. more nearby water tanks that may reflect/leak neutrons,
- the uncertainty/inaccuracies in the cross-section database if there are any,
- thermal effect that may not be accounted for yet, e.g. when boiling/heating up the water density will decrease, which may lead to less absorption, increasing the k_{eff} ,
- chemical interaction of various materials inside the set-up which may change the distribution of materials, e.g. corrosion may lead to leakage of water which may have acted as an absorber.

To allow room for such uncertainties, the simulation was re-done using a more conservative set-up through using a higher enrichment of uranium in all cylinders to simulate breeding of more fissile species. (A more accurate but unconservative approach is to raise the enrichment fraction for the central cylinder only.) As expected, the k_{eff} increased up to 1.06627 ± 0.00045 when the enrichment increased up to 25%, since more neutrons are absorbed by fissile atoms causing fission. However an addition of boron at $\approx 0.3\text{wt.}\%$ (i.e. 3000ppm, similar magnitude to those found in PWRs) was already sufficient to decrease the k_{eff} down to 0.76681 ± 0.00063 .

Subsequent iterative simulations with decreasing boron concentration shows that

- The magnitude of combined k_{eff} variation between cycles is larger compared to the case when no boron was present, possibly due to the increased number of neutrons being absorbed by the boron in water;
- The computing time per cycle decreased, likely due to the lowered k_{eff} ;

This leads to the decisions to

- increase the total number of cycles to 800 to reduce the uncertainty on k_{eff} such that a lower minimum concentration of boron can be used while maintaining sufficient confidence that it will keep the $k_{\text{eff}} < 0.8$
- doubling the number of particles per cycle to 10,000 to counteract the increased uncertainty introduced by the absorbing power of boron
- increase the number of cycle skipped at the beginning to 100 to account for the slower convergence due to the increased cycle-to-cycle fluctuation in k_{eff}

Which still leads to an acceptable computing time of < 8 minutes per simulation.

The 3σ envelope of k_{eff} was found to remain under 0.8 when boron concentration $> 1398.04\text{ppm}$ (input file's unnormalized weight fraction of boron $= 0.14\%$ times the water's weight fraction), giving $k_{\text{eff}} = 0.79766$, 3σ envelope ranges from 0.79677 to 0.79854; any lower (i.e. at 1298.31ppm) and the 3σ confidence interval begins to cross over the $k_{\text{eff}} > 0.8$ threshold, i.e. there will be a larger than 0.0675% chance of its $k_{\text{eff}} > 0.8$ (See Figure 1). See in table 5 in the Appendices for more.

5 Conclusion

In Exercise 1 the fluence was observed to decrease with distance of the tallying surface, in line with the results predicted when taking into account the inverse-square law and the neutron absorbing ability of water. When using $\text{nps}=2,800,000$ to model a 10^{10}s^{-1} neutron source using a point source at 2cm above the centre of the internal base of the bath, the average fluxes on the base, the long sides, and the short sides of the tank were recorded as $(3.4488 \pm 0.00344882) \times 10^7$, $(7.6834 \pm 0.00768341) \times 10^6$, and $(2.5094 \pm 0.00677549) \times 10^6\text{cm}^{-2}\text{s}^{-1}$; since, the fluence of these three tallies are given as 9656.7 ± 9.7 , 2151.4 ± 2.2 , and 702.6 ± 1.9 neutrons s^{-1} after 2,800,000 histories. The neutron spectra is also shown to have more thermalized neutron and fewer prompt, unmoderated neutrons when distance increases.

This analysis is quite reliable due to its small relative error and passing of all statistical tests. However in reality it might deviate from the simulation since a true point source is difficult to introduce.

In Exercise 3 the set-up was found to converge on $k_{\text{eff}} = 1.01798 \pm 0.00046$ when $e=20\%$ after running 500 cycles of NSRCK=5000 particles, skipping the first 10. It shows decreasing error on the combined k_{eff} as the simulation progresses; in order to keep $k_{\text{eff}} < 0.8$ when $e=25\%$, $\geq 0.139804\text{ wt.}\%$ boron should be added to the water, so that the 3σ 's envelope for k_{eff} is below 0.8, i.e. probability of $k_{\text{eff}} > 0.8$ is $< 0.0675\%$. To be more precise, the value of k_{eff} is given as 1.01798 ± 0.00033 , obtained after running the simulation at an increased source particle per cycle of NSRCK=10000, skipping more cycles (IKZ=100) at the beginning, while keeping the number of cycles ran to be the same (KCT=500).

One can be quite certain about the veracity of these simulations because sourcer particles were present in all fissile bodies, and the average combined k_{eff} converged in an expected manner without noticeable trend in the second half of the simulation. However, these simulations do not take into account the transmutation of elements, external sources of neutrons, and any other macroscopic effects which may perturb the distribution of materials inside the tank, so one has to be careful about these when applying these results to real life situations.

Appendices

A Figures

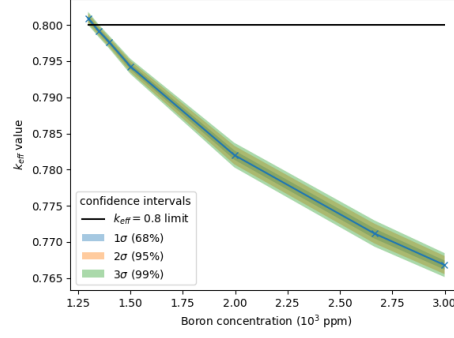


Figure 1: The k_{eff} only remains below 0.8 at boron concentration $\approx < 1400$ ppm. The data used is tabulated in table 5

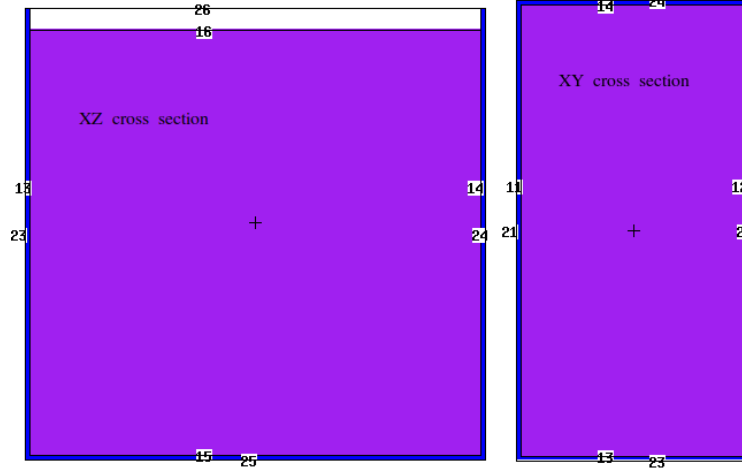


Figure 2: The XZ and XY cross section of the bucket at the origin ($y=0$ and $z=0$ respectively)

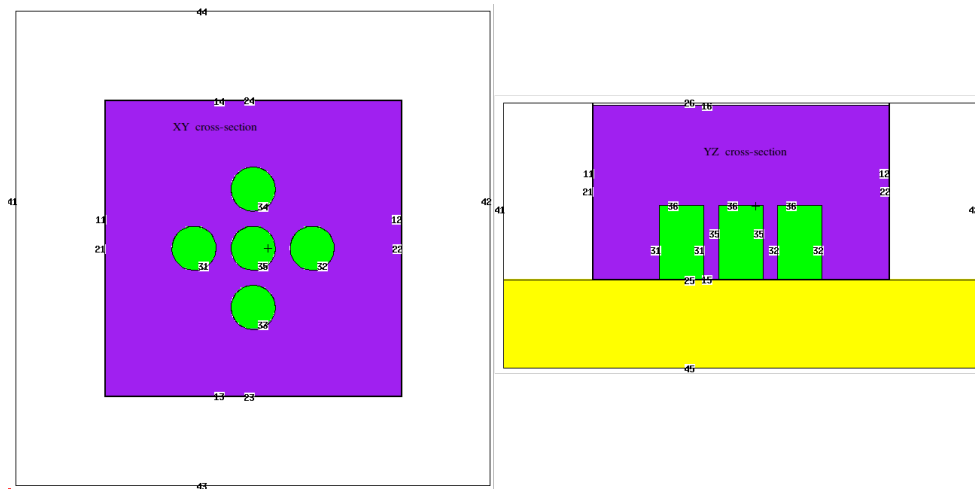


Figure 3: The XY and YZ cross section of the bucket at the origin ($z=0$ and $x=0$ respectively)

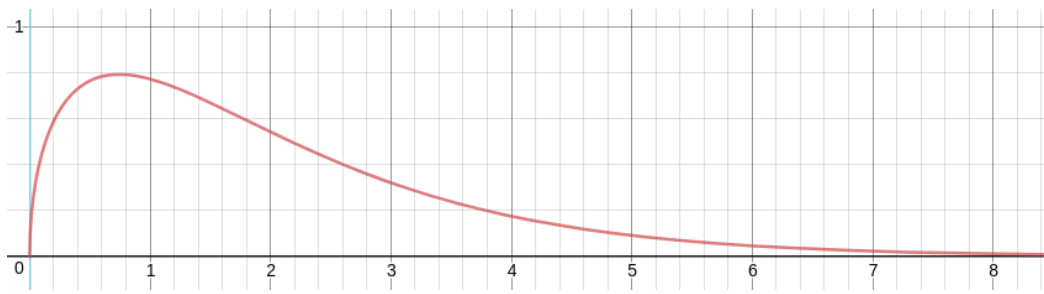


Figure 4: Watt Spectrum ($f=-3$) using the parameters $a=0.988, b=2.249$ for fission of ^{235}U by thermal neutron; note the diminishing but non-zero probability of emission of high energy particles. The x y axes have units of MeV and MeV^{-1} respectively

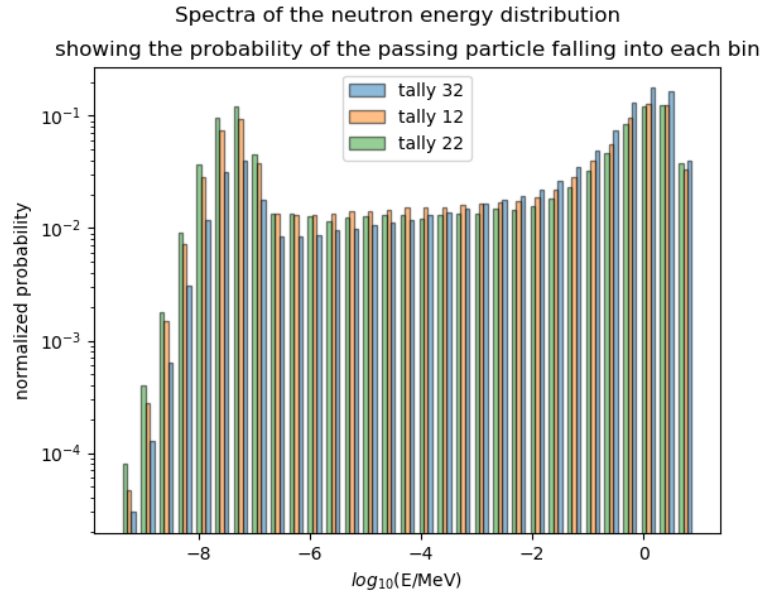


Figure 5: Probability of the passing particles falling into each of the 31 bins (which are evenly spaced on the log scale). y-axis of this graph is on log-scale.

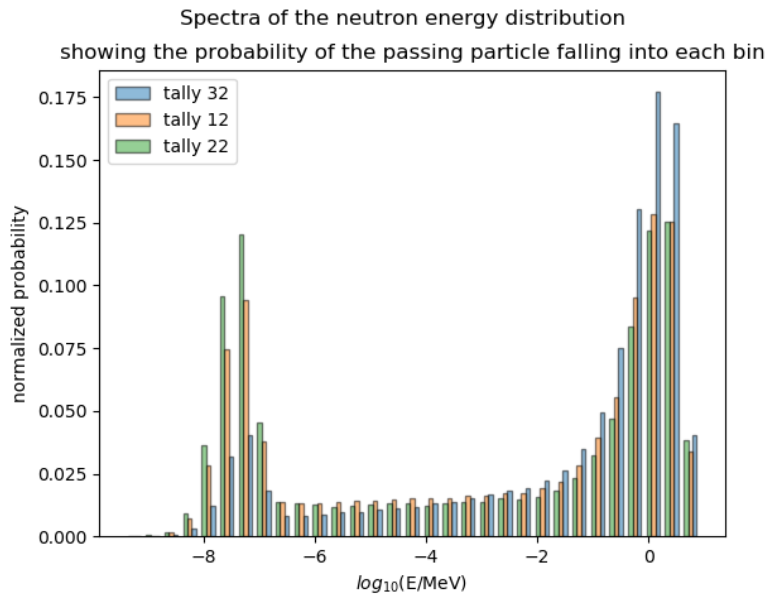


Figure 6: Same as figure 5 above, but with linear y-axis scale.

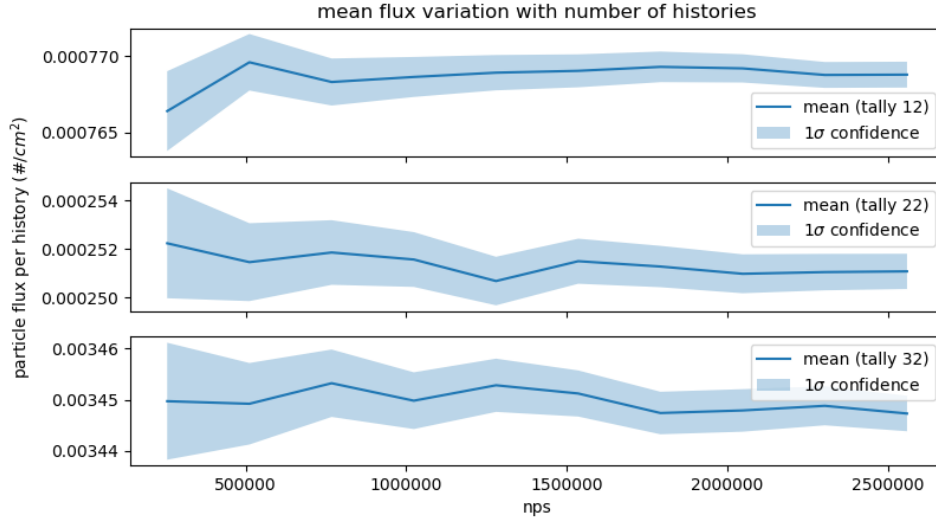


Figure 7: The mean and standard deviation on the mean retrieved from the tally fluctuation chart.

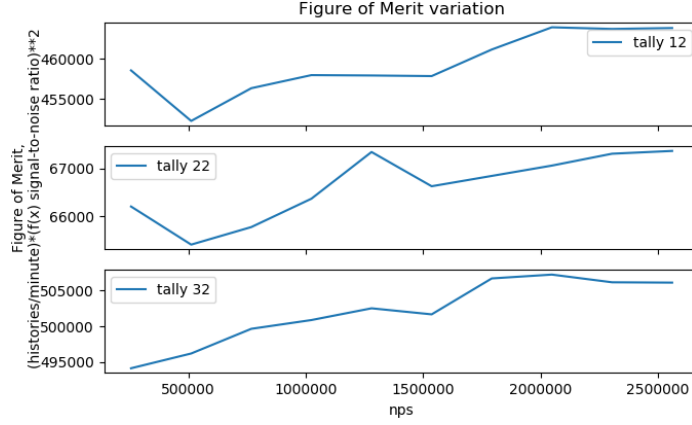


Figure 8: Flucation of Figure of Merit= $\frac{\text{histories}}{\text{minute}}(f(x)\text{signal-to-noise ratio})^2$ throughout the simulation.

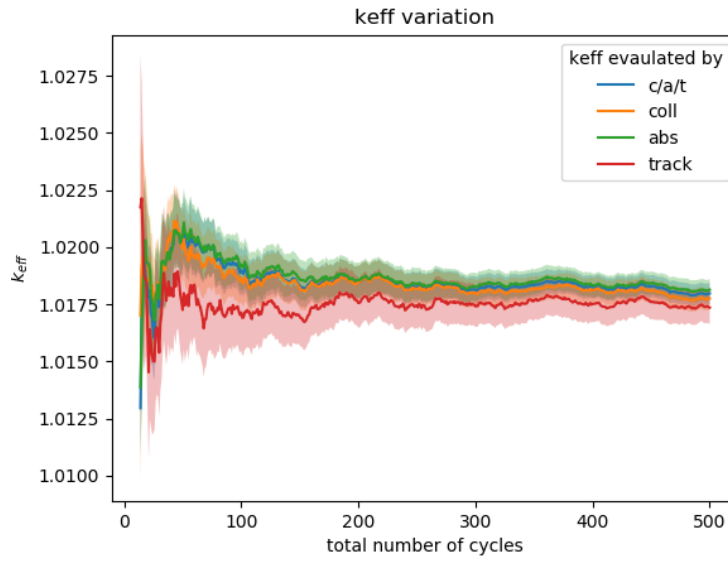


Figure 9: Plot of the average k_{eff} obtained by various methods, and including the 1σ (66%) confidence interval in the plot. Simulation completed using KCODE 5000 1 10 500

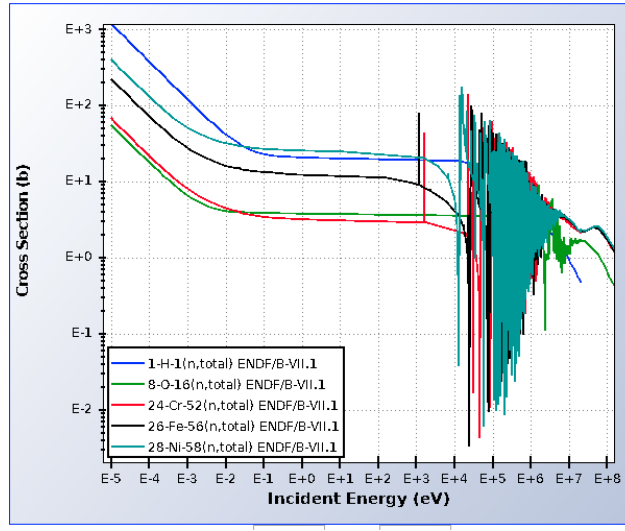


Figure 10: Variation of microscopic cross-section of all major isotopes that makes up the water and stainless steel wrt. energy, retrieved from [5].

B Tables

	water		stainless steel		concrete		U (e=20%)		U (e=25%)	
wt. %	^1_1H	11.1894	$^{nat}_{26}\text{Fe}$	74	$^{16}_8\text{O}$	53	$^{235}_{92}\text{U}$	20	$^{235}_{92}\text{U}$	25
	$^{16}_8\text{O}$	88.8106	$^{nat}_{24}\text{Cr}$	18	$^{nat}_{14}\text{Si}$	34	$^{238}_{92}\text{U}$	80	$^{238}_{92}\text{U}$	75
			$^{nat}_{28}\text{Ni}$	08	$^{nat}_{20}\text{Ca}$	10				
					^1_1H	03				
density ρ (g/cc)	1.00		7.92		2.30		19.20		19.20	

Table 3: Isotopic compositions and density of all materials used; data for water is given by [4]
 nat refers to naturally occurring element's isotopic compositions.

tally (surface(s))	12 (long sides of the tank)	22 (short sides of the tank)	32 (base of the tank)
Flux ($\text{cm}^{-2}\text{s}^{-1}$) extrapolated from the 20,000 nps simulation	7480000 \pm 90000	2398000 \pm 8000	34200000 \pm 400000
Flux ($\text{cm}^{-2}\text{s}^{-1}$) extrapolated from the 2,800,000 nps simulation	7683000 \pm 7700	2509000 \pm 6800	34490000 \pm 34000
Flux ($\text{cm}^{-2}\text{s}^{-1}$) extrapolated from the 18,000,000 nps simulation	7681000 \pm 3000	2505000 \pm 2800	34560000 \pm 14000

Table 4: Flux expected from a 10^{10}s^{-1} point source of neutron placed at the same location, predicted from the 20,000 neutrons, 2,800,000 neutrons, and 18,000,000 neutrons simulations respectively. One can see that the result from Tally 32 converged to a stable value early on (in the nps=20,000 simulation); but the other two requires much more number of histories to reach their asymptotic limits. The 1st bins of tallies 12 and 22 still have relative errors > 0.1 after the nps=2,800,000 simulation; so in theory the values were not accurate enough yet; but as seen in the table, this contributed negligibly to the total fluence because so few particles can reach the 1st bin of tallies 12 and 22; thus the predicted fluences contributed by thoes two bins do not differ much even after those two bins are forced to converge by sextupling the number of histories to nps=18,000,000.

Boron concentration (wt.%)	0.129831	0.134982	0.139804	0.1499778	0.199601	0.266439	0.299910
$k_{\text{eff}}+3\sigma$	0.80182	0.80003	0.79854	0.79532	0.78371	0.77298	0.76846
$k_{\text{eff}}+2\sigma$	0.8016	0.79982	0.79832	0.79506	0.78329	0.77253	0.76806
$k_{\text{eff}}+1\sigma$	0.80126	0.79949	0.79799	0.79467	0.78265	0.77185	0.76743
k_{eff}	0.80091	0.79916	0.79766	0.79427	0.78201	0.77117	0.76681
$k_{\text{eff}}-1\sigma$	0.80057	0.79883	0.79732	0.79387	0.78137	0.77048	0.76618
$k_{\text{eff}}-2\sigma$	0.80022	0.79851	0.79699	0.79347	0.78073	0.7698	0.76556
$k_{\text{eff}}-3\sigma$	0.80000	0.79829	0.79677	0.79322	0.78031	0.76935	0.76515

Table 5: Variation in k_{eff} wrt. boron concentration in water. All simulations were completed using KCODE 10000 1 100 500

C References

- [1] MCNP4C2: Monte Carlo N-Particle Transport Code System Abstract (Diagnostics Applications Group, Los Alamos National Laboratory, Los Alamos, New Mexico.) p.2-160 (June 2001.)
- [2] MCNP4C2: Monte Carlo N-Particle Transport Code System Abstract (Diagnostics Applications Group, Los Alamos National Laboratory, Los Alamos, New Mexico.) p.4-30 (June 2001.)
- [3] MCNP4C2: Monte Carlo N-Particle Transport Code System Abstract (Diagnostics Applications Group, Los Alamos National Laboratory, Los Alamos, New Mexico.) p.2-180 (June 2001.)
- [4] Compendium of Material Composition Data for Radiation Transport Modeling (R.G. Williams III, C.J. Gesh, R.T. Pagh) p.111 (April 2006)
- [5] Brown, D., Sonzogni, A. and Pritychenko, B. (2011). Sigma Periodic Table Browse. [online] Nndc.bnl.gov. Available at: <http://www.nndc.bnl.gov/sigma/index.jsp> [Accessed 22 Apr. 2019].